Journal of Physics: Conference Series

PAPER • OPEN ACCESS

Influence of platform motion on the energy production of a floating wind farm

To cite this article: M. De Pascali *et al* 2024 *J. Phys.: Conf. Ser.* **2767** 092046

View the article online for updates and enhancements.

You may also like

- Numerical Study of Typhoon Resistance of a Floating Wind Turbine
Liwei Zhang, Boyuan Qiu, Li Ren et al.
- Experimental Analysis of the Wake Meandering of a Floating Wind Turbine under Imposed Surge Motion
L. Pardo Garcia, B. Conan, S. Aubrun et al.
- The potential role of airborne and floating wind in the North Sea region
Hidde Vos, Francesco Lombardi, Rishikesh Joshi et al.

This content was downloaded from IP address 141.70.168.7 on 11/06/2024 at 14:27

Journal of Physics: Conference Series **2767** (2024) 092046 doi:10.1088/1742-6596/2767/9/092046

Influence of platform motion on the energy production of a floating wind farm

M. De Pascali, A. Fontanella, S. Muggiasca, M. Belloli

Dept. of Mechanical Engineering, Politecnico di Milano, via La Masa 1, 20156 Milano, Italy.

E-mail: alessandro.fontanella@polimi.it

Abstract. This study investigates the dynamics of energy production in floating wind farms. Unlike their bottom-fixed counterparts, floating wind turbines experience large-amplitude, low-frequency movements affecting the rotor response and the wake development. We employed the multi-physics simulator FAST.Farm to study a seven-turbine wind farm, comparing conventional monopile foundations with semi-submersibles. Results show that, under undisturbed wind conditions, floating turbines exhibit a lower power-conversion efficiency due to platform tilt and the use of a thrust clipping controller. Conversely, waked turbines in a floating configuration have a higher power output than with a bottom-fixed foundation. This is attributed to the higher wind speed in their wake which is due to the lower thrust set point of the floating controller, the vertical deflection of the wake and the dynamic conditions at rotor created by motion.

1. Introduction

In recent years the first utility-scale floating wind farms have been installed and others are expected to go online in the next future. Foundation compliance in a floating wind turbine (FOWT) allows large-amplitude low-frequency motions which interact with the wind turbine controller, influence in a significant manner the wind speed experienced by rotor and affect the wake development. Due to these differences with respect to bottom-fixed offshore turbines, it is crucial to understand the physics of the energy conversion process taking place in floating wind farms to quantify their energy production with low uncertainty.

Recent studies have shown that waves excitation has negligible effects on the power output of an isolated floating wind turbine [1, 2], but there is no research addressing the energy production of floating wind farms. The low-frequency movement of a FOWT can modify the turbine wake and its propagation downstream. This has been shown with a vortex method in [3], and computational fluid dynamics simulations in [4], where it is found the floater motion triggers a faster breakdown of the wake. Wakes, and the associated losses, are a driving factor in the energy production of wind farms [5], hence it is reasonable to expect the different wake behavior can introduce variations in the power output when bottom-fixed foundations are replaced with floating platforms.

In this study, we use multi-physics wind farm simulations to investigate the energy production in floating wind farms, in particular how this is influenced by the low-frequency motions of FOWTs support platforms. To answer this question, we model in FAST.Farm two small wind farms, each of seven 15 MW wind turbines, one with monopile foundations and one with semi-submersible platforms.

Content from this work may be used under the terms of the Creative Commons Attribution 4.0 licence. Any further distribution of this work must maintain attribution to the author(s) and the title of the work, journal citation and DOI.
Published under licence by IOP Publishing Ltd

Section 2 describes the structure of FAST.Farm and how the software accounts for wake dynamics due to movements of floating platforms. The wind farms, the environmental conditions, and the simulations setup are explained in Sect. 3. Results of simulations are presented and discussed in Sect. 4, followed by the conclusions and suggestions for future work in Sect. 5.

2. Simulations tools

The wind farms are simulated in FAST.Farm, which is a mid-fidelity nonlinear time-domain multi-physics engineering tool developed by NREL for predicting wind turbines power performance and structural loads within a wind farm [6, 7]. FAST.Farm has been recently used for load analyses of floating wind farms: in [8] a two-turbine floating wind farm is examined showing wake meandering can excite the rigid-body movements of the platform with increased fatigue loads for the wind turbine components.

FAST.Farm combines three main modules: OpenFAST and its sub-modules, WakeDynamics, and the Ambient Wind and Array Effects (AWAE) module.

- OpenFAST models the aero-hydro-servo-elastic response of a wind turbine receiving the inflow from AWAE;
- WakeDynamics models the wake of a wind turbine, including wake advection, deflection, and meandering, a near-wake correction and a wake-deficit increment;
- AWAE models the wind inside the wind farm array merging a turbulent background flow and wind turbines wakes.

FAST.Farm invokes one instance of OpenFAST and one of WakeDynamics for every wind turbine in the wind farm. The background turbulent wind field is obtained with the stochastic, full-field, turbulent-wind simulator TurbSim [9].

The rotor of a floating wind turbine undergoes large motions due to the compliance of the support platform. The effect of these movements on the wake evolution is modelled in WakeDynamics as exemplified in Fig. 1. In WakeDynamics, the wake is calculated in a discrete number of wake planes. At every time step, one plane is emitted by the wind turbine rotor and the other planes forming the wake are convected downstream using the inflow velocity computed in AWAE. The wake deficit on the rotor plane is computed based on the filtered thrust coefficient computed in OpenFAST. The wake deficit evolution on the discrete planes is obtained solving the thin shear layer approximation of the Navier-Stokes equation. With this approach the wake-deficit evolves based on the local conditions at rotor, accounting for transients in the inflow, turbine control and, importantly for this study, turbine motions. The local conditions at the rotor undergo low-pass filtering to capture the time it takes for the wake to respond.

AWAE uses multiple domains to compute the wind inflow. A 3D grid of nodes, called low-resolution domain, covers the entire wind farm and has a node spacing of 35 m and wind is updated every 0.4 s. Around each turbine there is a higher resolution grid with a node spacing of 5 m and wind is updated every 0.02 s.

3. Floating wind farm scenario and simulation setup

The wind turbine and the two foundations we considered are described in Sect. 3.1, the wind farm layout is presented in Sect. 3.2, the met-ocean conditions in Sect. 3.3, the simulations setup is summarized in Sect. 3.4.

3.1. Wind turbine

The wind turbine is the IEA 15 MW [10]. It has a rotor diameter (D) of 240 m and a hub height of 150 m. The wind turbine has a conventional variable-speed, variable blade-pitch-to-feather control configuration, a rated wind speed of 10.59 m/s, and a rated rotor speed of 7.56 rpm.

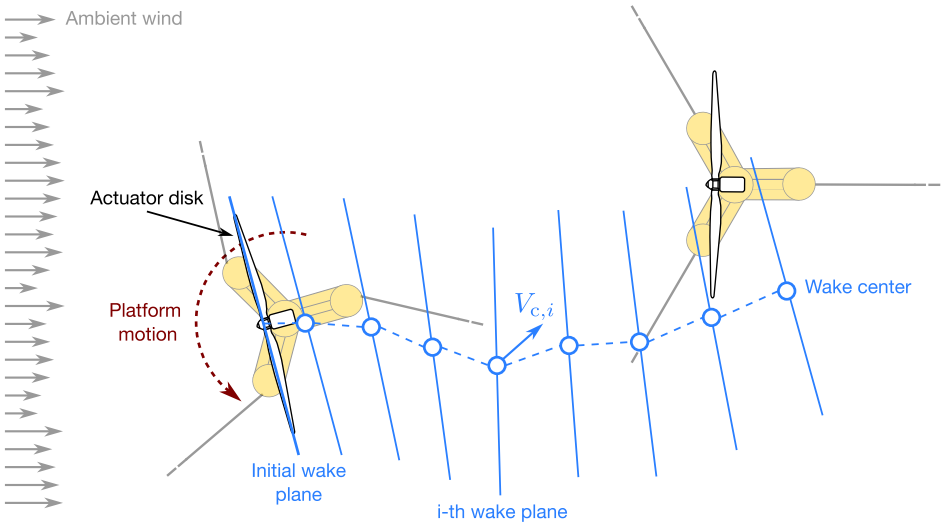

Figure 1. Wake evolution in FAST.Farm. The wake is calculated on discrete wake planes emitted from a wind turbine rotor. The wake on the initial plane considers the rotor local conditions such as the rigid-body movement of the platform. Wake planes are convected downstream with the local inflow velocity at the wake center $V_{c,i}$.

Two different foundations have been considered: a monopile and the VolturnUS semi-submersible platform. The monopile [10] is a steel tube of 10 m diameter, the first tower-monopile mode occurs at a frequency of 0.17 Hz. The VolturnUS floater [11] is a steel platform composed of three 12.5 m diameter columns disposed symmetrically around a central column hosting the wind turbine. The mooring system is designed for a generic 200-m-depth location and is composed of three 850 m long chain-catenary lines, arranged at 120° angle around the floater.

The wind turbine power-production operation is controlled with the NREL Reference Open-Source Controller (ROSCO) [12]. In below rated wind speeds the blade pitch is fixed to its design value of 0° and a proportional-integral controller regulates the generator torque to track the design tip-speed ratio. In above rated wind speeds the generator torque is constant and equal to its rated value while the rotor speed is regulated with a proportional-integral controller on the collective blade pitch angle. The nacelle-yaw angle is constant in time, but motions of the floating platform induce relative misalignment between the rotor and the incoming wind as depicted in Fig. 1.

In the semi-submersible case, a peak shaving control algorithm has been adopted. This additional ROSCO functionality reduces the maximum thrust force in near-rated winds prescribing a minimum blade pitch $> 0°$ function of the wind speed.

3.2. Wind farm layout

The wind farm layout is a seven-turbines subset of the TotalControl Reference Wind Power Plant [13]. The TotalControl power plant has 32 wind turbines organized in staggered rows and columns separated by a 5D distance. It is recommended for benchmark studies on wind power plant control because it has compact spacing that emphasize wake interactions and the efficacy of wake flow control actions. The plant is designed with symmetry to facilitate simulations and it has a recurrent hexagonal pattern of seven turbines, shown in Fig. 2, which is the object of this study.

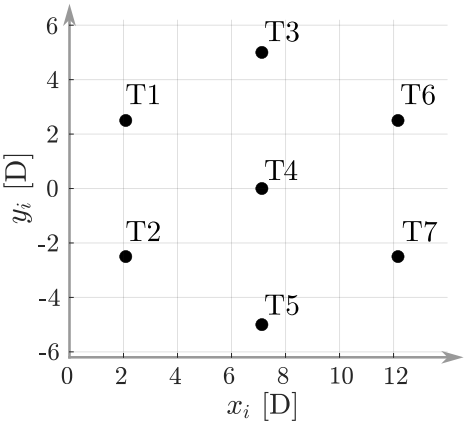

Figure 2. Position of the wind turbines (T) in the wind farm.

3.3. Environmental conditions

We examined one below rated scenario with a mean wind speed of 10 m/s because in this condition wind turbines are operated at nearly maximum thrust and wake effects are significant. 16 wind directions (φ) equally spaced of 22.5° are considered.

The wind fields of the simulations are generated in TurbSim. The wind is calculated based on the Kaimal turbulence model, the turbulence intensity is 0.12, the wind speed vertical profile follows a power law with a shear exponent of 0.14. Waves in the simulations are of irregular type based on the JONSWAP spectrum. The wave height and the peak spectral period are defined from linear correlation with the average wind speed following the same procedure of [2], resulting in a $H_\mathrm{s} = 2$ m and a $T_\mathrm{p} = 5.5$ s. Only aligned wind/wave conditions have been considered.

3.4. Simulation setup

Each FAST.Farm simulation has a time length of 4200 s, the first 600 s were discarded in the post-processing to remove transient effects, resulting in an effective simulation length of 1 hour which is necessary to capture the slow dynamics of the floating foundation. Six 1-hour simulations with different realizations of the turbulent wind field and waves are run for every wind direction to reproduce the stochastic variability of environmental excitation.

The OpenFAST model of each wind turbine includes modules for aerodynamics, hydrodynamics, control, and structural dynamics [14]. The aerodynamic forces are calculated in AeroDyn v15 based on the quasi-steady blade element momentum theory. Hydrodynamic loads are evaluated in HydroDyn combining potential-flow theory for radiation/diffraction effects and strip-theory for viscous drag. The mooring lines of the semi-submersible are modeled in MoorDyn using a lumped-mass approach. The structural response of the system is calculated in ElastoDyn with multi-body theory and the modal approach. Each OpenFAST instance in FAST.Farm has a time step of 0.1 s.

4. Results and discussion

Power production at farm level is affected by the behavior of individual wind turbines. In Sect. 4.1 we show the use of a floating platform modifies the steady-state response of a wind turbine rotor. These differences at the turbine level combine with those rising at the farm level due to wakes, and this is presented in Sect. 4.2.

4.1. Response of the isolated wind turbine

The steady-state operating points of generated power and rotor aerodynamic thrust force of the IEA 15 MW, with monopile foundation and the VolturnUS semi-submersible, regulated with the control strategy described in Sect. 3.1, are visualized in Fig. 3. The peak-shaving routine of the floating wind turbine controller reduces the maximum thrust force near the rated wind speed at the expense of a lower generated power. At 10 m/s, the peak shaving reduces the thrust force of 10% compared to the monopile case and due to the momentum conservation, this leaves a slightly larger amount of kinetic energy in the wind turbine wake.

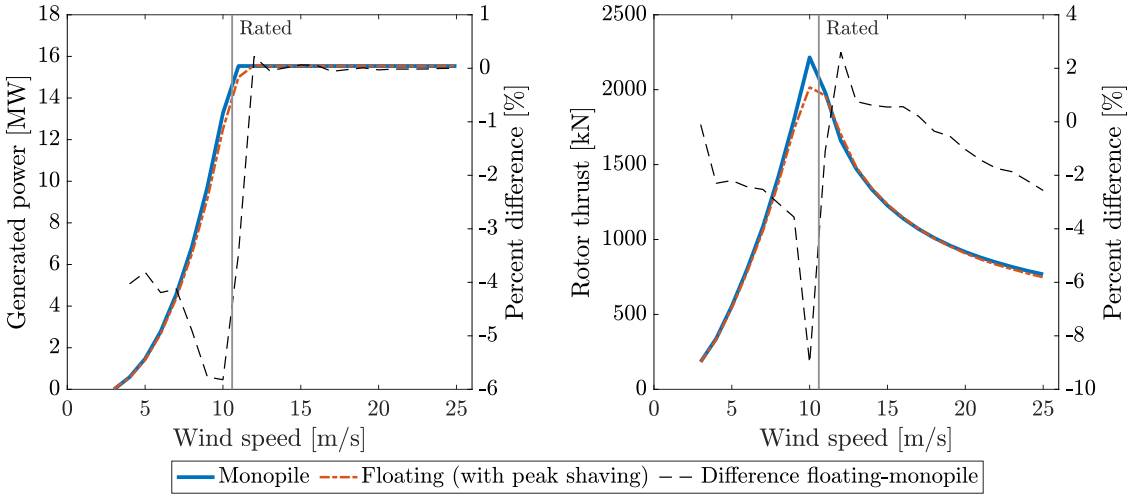

Figure 3. Steady-state power curves of generated power and rotor aerodynamic thrust force of the wind turbines with monopile and floating foundations. The floating wind turbine controller has a peak shaving routine limiting the maximum thrust force at the expense of a lower power output.

In the below-rated region, the thrust force and generated power are lower for the floating wind turbine compared to the monopile case. This is due to the platform static tilt and the consequent reduction of rotor area projection on the vertical plane. In the above-rated region, the generated power is saturated to its rated value and is equal for the monopile and floating wind turbines. The thrust force is slightly higher for the floating wind turbine compared to the monopile for wind speeds just above rated, and is lower for higher wind speeds.

4.2. Response of the wind farm

The symmetry of the wind farm layout is reflected in the generated power that has a similar behaviour in the four quadrants of the wind direction. In the first quadrant ($0° \leq \varphi \leq 90°$) we distinguish three situations that are summarized in Table 1. For $\varphi = 0°$, the monopile wind farm exhibits a similar power compared to the floating wind farm; when $\varphi = 45°$, the monopile wind farm exhibits a higher power; when $\varphi = 90°$, the monopile wind farm exhibits a lower power.

The contributions of individual wind turbines to the total generated power is examined in Fig. 4. We distinguish two situations: some turbine units generate a power close to 12 MW, corresponding to the output of the isolated case (see Fig. 3), whereas others, that are waked, have a reduced power output. In the first condition, the generated power with a floating platform is lower than with a monopile, and this is attributed to the wind turbine static tilt. In the other case it is the opposite: the floating wind turbines produce more power. To explain the differences

Table 1. Power generated by the bottom-fixed and floating wind farms obtained averaging the 6 simulations with different realization of stochastic wind and waves for every wind direction.

Wind direction [°]	Power monopile [MW]	Power floating [MW]
0	78.86	77.97
45	87.88	84.29
90	58.64	60.88

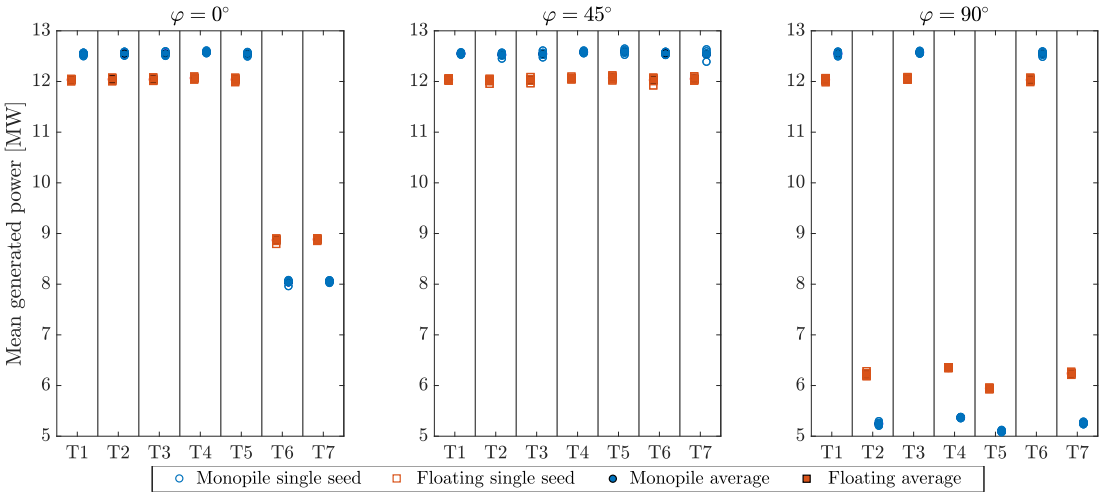

Figure 4. Power generated by the seven wind turbines (T), in the monopile and floating cases, for three wind directions φ.

in terms of power generated by the waked wind turbines we analyze the wake losses and their impact on the energy-conversion process at rotor level.

Wake losses depend on the wind direction since for some incoming wind angles there are turbines working in a more pronounced waked condition. This is visualized in Fig. 5 showing the instantaneous flow field across the farm for $\varphi = 0°$. For $\varphi = 90°$ four wind turbines (T2, T4, T7, T5) operate in the wake of upstream units, for $\varphi = 0°$ two wind turbines (T6, T7) are waked, when $\varphi = 45°$, wakes are directed between rotors of downstream units and there are no wake losses. For $\varphi = 45°$ the response of the isolated turbine drives the wind farm performance, while for $\varphi = 0°$ or $90°$ wakes affect the power production of some units, triggering a different behavior of floating wind turbines compared to bottom-fixed ones.

Figure 5 shows the longitudinal wind speed in the turbine wakes is generally higher for the floating wind farm compared to the monopile case. The higher wind speed in the wake of floating wind turbines is mainly due to these factors: slightly less energy is extracted from the flow with peak shaving; the large low-frequency motions of the floating platform affect the wake meandering; the wake is deflected upwards due to the increased rotor tilt given by platform static pitch.

The wake meandering is examined in Fig. 6 showing the standard deviation of the lateral wake center position at a distance of 5D from the rotor, for the seven turbines, in the monopile and floating cases. The general trend is that wakes oscillate with larger amplitudes in the side-to-side direction in the floating wind turbines than in those with a monopile foundation. Although FAST.Farm has not been validated yet with respect to the wake development in floating wind

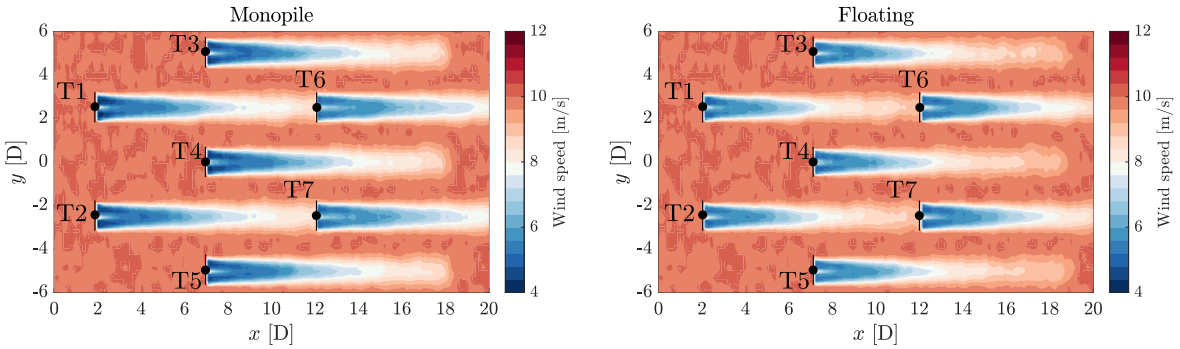

Figure 5. Time averaged flow fields of longitudinal wind speed across the wind farm, on a plane at 150 m from the water level, for the monopile and floating foundations with wind coming from $\varphi = 0°$.

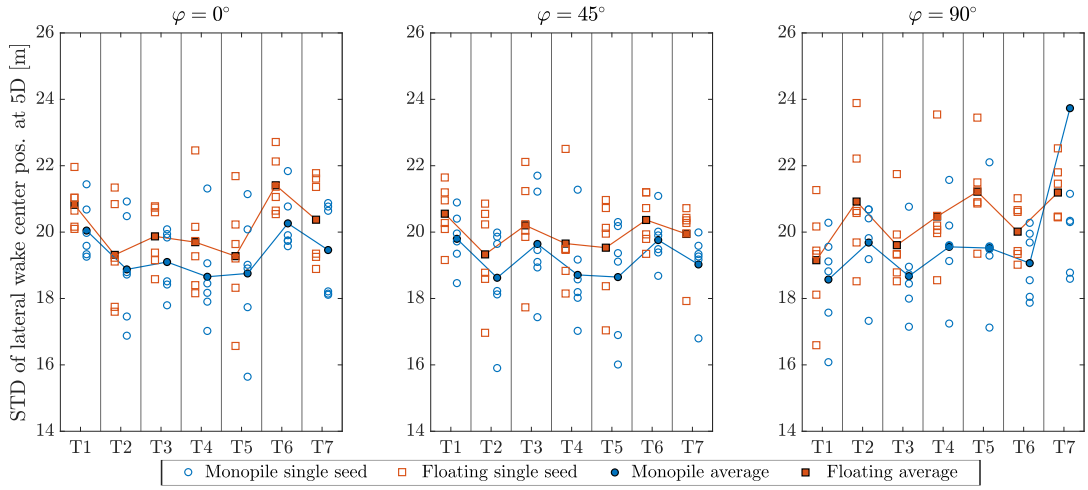

Figure 6. Standard deviation of the lateral wake center position at a distance of 5D from the rotor, for the seven wind turbines (T), in the monopile and floating cases, for three wind directions φ.

turbines, the tendency of a FOWT to have a more accentuated wake meandering due to its side-to-side motion has been recently found in few studies [3, 4].

We checked the correlation of the platform side-to-side motions with the wake development examining the spectrum of the lateral motion of the wake center of turbine T1. This is shown in Fig. 7 for a downstream distance of 5D, comparing the floating and monopile cases. The lateral motion of the wake center exhibits a larger amount of spectral energy compared to the monopile at the natural frequencies of the FOWT rigid-body motion modes. The wake moves more at frequencies corresponding to the surge, yaw, pitch, and roll motions which seem to trigger an increased wake meandering in FAST.Farm.

In the floating case, the low-frequency motion of the rotor and the use of peak shaving may leave more energy in the wake compared to the monopile case. This is explored in Fig. 8 which shows the mean wind speed (ambient wind disturbed by wakes) at hub-height for three wind directions, with monopile and floating wind turbines. For $\varphi = 0°$, T6 and T7 experience the wake of upstream wind turbines; for $\varphi = 90°$ T2, T4, T5, and T7 are in waked condition; for $\varphi = 45°$ wake effects are minimized by the layout geometry and all wind turbines experience the free stream wind speed. In general floating wind turbines in waked conditions experience a

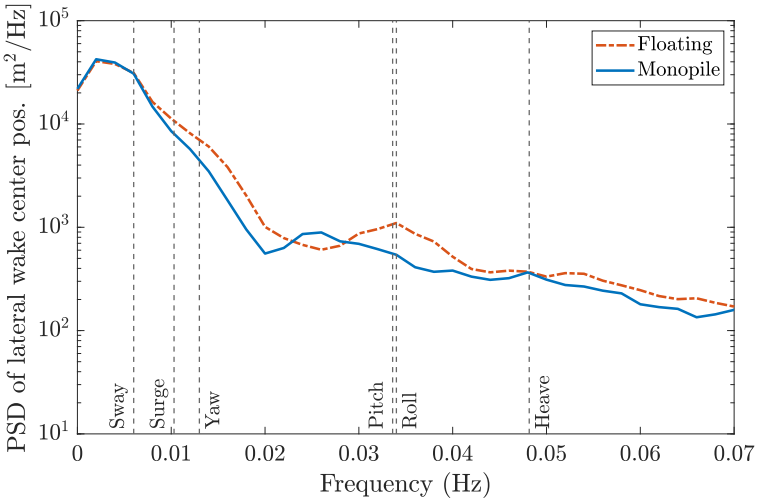

Figure 7. Power spectral density of the lateral wake center position at 5D from the rotor of the turbine T1 with a monopile and a floating foundations. The vertical dashed lines are in correspondence of the natural frequencies of the rigid-body motions of the floating wind turbine.

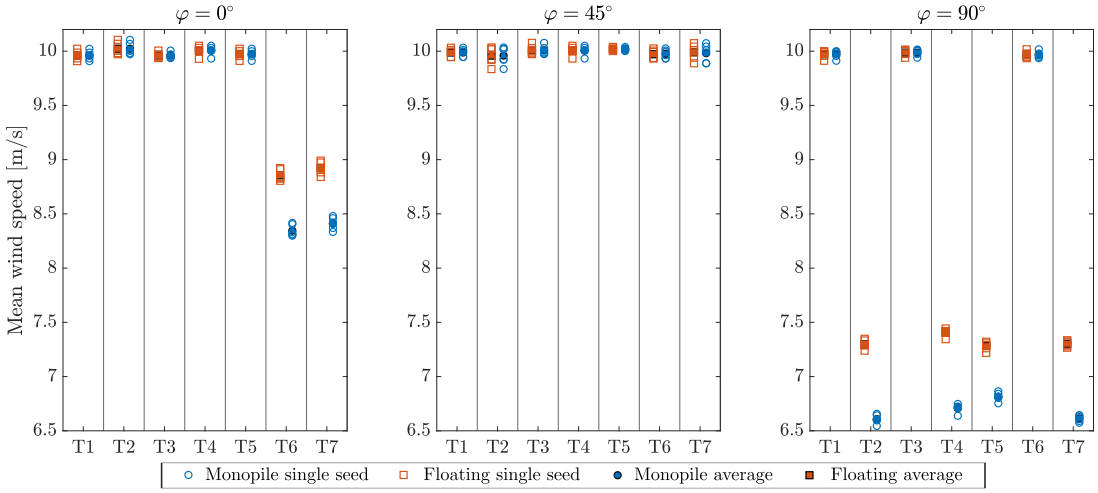

Figure 8. Mean wind speed at hub height for the seven wind turbines (T), in the monopile and floating cases, for three wind directions φ.

higher mean wind speed compared to the monopile case.

The mean power generated by the wind turbines, which is reported in Fig. 4, follows approximately the same trend of the mean wind speed of Fig. 8. When operating in an undisturbed wind field (i.e., with a wind speed of 10 m/s) the monopile wind turbines exhibit a larger generated power. This is because they have a better efficiency compared to the floating case: they do not use the peak shaving controller and do not suffer of the reduction of rotor area projection on the plane normal to wind. Conversely, when in the wake of an upstream unit, floating wind turbines produce more power. Although they have a lower efficiency, this is offset by the higher wind speed they experience.

5. Conclusions

In this study, we investigated the energy production of a small floating wind farm and how this is influenced by the low-frequency movements of floating foundations. We modeled a seven-turbine wind farm in the multi-physics simulator FAST.Farm and we studied how the farm response changes when conventional bottom-fixed foundations are replaced with semi-submersibles. Our results show that, when operating in an undisturbed wind, floating wind turbines have a lower power-conversion efficiency compared to their bottom-fixed equivalent. This is due to the reduction of rotor area projection normal to wind caused by the floater tilt and the use of a peak-shaving control strategy. However, a reverse trend has been found for waked wind turbines, that exhibit a higher power output in the floating case. We linked the higher generated power of waked floating turbines to the higher wind speed found in their wake, which is mainly due to dynamic conditions at rotor created by platform motion, the wake upward deflection associated with platform static tilt, and the use of a thrust clipping controller. Furthermore, it is shown that the low-frequency movements of floating wind turbines cause a more pronounced wake lateral wake meandering than with a monopile foundation.

Although it is suggested by standards, the wind turbulence intensity we modeled in our simulations is high for an offshore site. Probably, with a lower turbulence, the effects of platform motion on the wind turbine wake would be even more pronounced. In this study, waves have been assumed to be aligned to the wind direction. Waves that are misaligned excite lateral movements in the floater, potentially amplifying wake meandering.

In future work it is advised to extend the analysis to more wind and wave scenarios that are closer to the operating conditions normally faced by a floating wind farm. Moreover, FAST.Farm has been validated for bottom-fixed wind farms against higher-fidelity models and in-field measurements, however it is yet to be proven if the wake evolution predicted by FAST.Farm in response to the motion of a floating wind turbine is adherent to reality.

References

[1] Saenz-Aguirre A, Ulazia A, Ibarra-Berastegi G and Saenz J 2022 *Energy Conversion and Management* **271** 116303 ISSN 0196-8904 URL https://www.sciencedirect.com/science/article/pii/S0196890422010810
[2] Fontanella A, Colpani G, De Pascali M, Muggiasca S and Belloli M 2023 *Wind Energy Science Discussions* **2023** 1–33 URL https://wes.copernicus.org/preprints/wes-2023-137/
[3] Ramos-García N, González Horcas S, Pegalajar-Jurado A, Kontos S and Bredmose H 2022 *Wind Energy* **25** 1434–1463 (*Preprint* https://onlinelibrary.wiley.com/doi/pdf/10.1002/we.2738) URL https://onlinelibrary.wiley.com/doi/abs/10.1002/we.2738
[4] Li Z, Dong G and Yang X 2022 *Journal of Fluid Mechanics* **934** A29
[5] Meyers J, Bottasso C, Dykes K, Fleming P, Gebraad P, Giebel G, Göçmen T and van Wingerden J W 2022 *Wind Energy Science* **7** 2271–2306 URL https://wes.copernicus.org/articles/7/2271/2022/
[6] Jonkman J and Shaler K 2021 Fast.farm user's guide and theory manual Tech. rep. National Renewable Energy Laboratory URL https://www.nrel.gov/docs/fy21osti/78485.pdf
[7] Branlard E, Martínez-Tossas L A and Jonkman J 2023 *Wind Energy* **26** 44–63 (*Preprint* https://onlinelibrary.wiley.com/doi/pdf/10.1002/we.2785) URL https://onlinelibrary.wiley.com/doi/abs/10.1002/we.2785
[8] Wise A S and Bachynski E E 2020 *Wind Energy* **23** 1266–1285 URL https://onlinelibrary.wiley.com/doi/abs/10.1002/we.2485
[9] Jonkman J Turbsim user's guide Tech. rep. National Renewable Energy Laboratory
[10] Gaertner E, Rinker J and Sethuraman L, Zahle F, Anderson B, Barter G, Abbas N, Meng F, Bortolotti P, Skrzypinski W, Scott G, Feil R, Bredmose H, Dykes K, Shields M, Allen C and Viselli A 2020 Available at https://www.nrel.gov/docs/fy20osti/75698.pdf URL https://www.nrel.gov/docs/fy20osti/75698.pdf
[11] Allen C, Viselli A, Dagher H, Goupee A, Gaertner E, Abbas N, Hall M and Barter G Definition of the UMaine VolturnUS-S reference platform developed for the IEA Wind 15-megawatt offshore reference wind turbine Tech. rep. International Energy Agency
[12] Abbas N J, Zalkind D S, Pao L and Wright A 2022 *Wind Energy Science* **7** 53–73 URL https://wes.copernicus.org/articles/7/53/2022/

[13] Andersen S, Madariaga A, Merz K, Meyers J, Munters W and Rodriguez C Advanced integrated supervisory and wind turbine control for optimal operation of large wind power plants Tech. rep. SINTEF Energy Research
[14] Jonkman B, Mudafort R M, Platt A, Branlard E, Sprague M, Jonkman J, Ross H, Hall M, Vijayakumar G, Buhl M, Bortolotti P, Ananthan S, Schmidt M, Rood J, Damiani R, Mendoza N, Shaler K, Housner S, Bendl K, Carmo L, Quon E, Phillips M R, Kusuno N and Salcedo A G 2023 Openfast/openfast: v3.4.1 URL `https://doi.org/10.5281/zenodo.7632926`